Familial Mutations and Zinc Stoichiometry Determine the Rate-Limiting Step of Nitrocefin Hydrolysis by Metallo-β-lactamase from *Bacteroides fragilis*†

Walter Fast, Zhigang Wang,‡ and Stephen J. Benkovic*

Department of Chemistry, The Pennsylvania State University, 414 Wartik Laboratory, University Park, Pennsylvania 16802

Received August 8, 2000; Revised Manuscript Received November 21, 2000

ABSTRACT: The diverse members of the metallo-β-lactamase family are a growing clinical threat evolving under considerable selective pressure. The enzyme from *Bacillus cereus* differs from the *Bacteroides fragilis* enzyme in sequence, zinc stoichiometry, and mechanism. To chart the evolution of the more reactive *B. fragilis* enzyme, we have made changes in an active site cysteine residue as well as in zinc content to mimic that which occurs in the *B. cereus* enzyme. Specifically, by introducing a C104R mutation into the *B. fragilis* enzyme, binding of two zinc ions is maintained, but the k_{cat} value for nitrocefin hydrolysis is decreased from 226 to 14 s^{-1}. Removal of 1 equiv of zinc from this mutant further decreases k_{cat} to 4.4 s^{-1}. In both cases, the observed k_{cat} closely approximates that found in the di- and monozinc forms of the *B. cereus* enzyme (12 and 6 s^{-1}, respectively). Pre-steady-state stopped-flow studies using nitrocefin as a substrate indicate that these enzyme forms share a similar mechanism featuring an anionic intermediate but that the rate-limiting step changes from protonation of that species to the C−N bond cleavage leading to the intermediate. Overall, features that contribute 3.7 kcal/mol toward the acceleration of the C−N bond cleavage step have been uncovered although some of the total acceleration is masked in the steady-state by a change in rate-limiting step. These experiments illustrate one step in the evolution of a catalytic mechanism and, in a larger perspective, one step in the evolution of antibiotic resistance mechanisms.

Widespread use of β-lactam antibiotics, originally by β-lactam producing organisms and more recently by humans in clinical settings and in animal feed, provides an incredible selective pressure that drives the evolution of antibiotic resistance mechanisms in bacteria (*1*−*3*). While numerous methods of resistance have emerged including mutation of penicillin binding proteins, alteration of membrane permeability, and even production of efflux pumps, one of the major clinical concerns has been the evolution of wide-spectrum β-lactamases which hydrolyze the antibiotic to an inactive form (*4*, *5*). Although the TEM-derived serine-based β-lactamases are currently considered the most clinically important among the extended-spectrum β-lactamases, metallo-β-lactamases (Class B or Class 3 lactamases) are of growing concern because they threaten rapid plasmid-encoded dissemination, they have an extremely broad substrate profile, and they are not inhibited by clinically useful inhibitors of serine β-lactamases such as clavulanic acid. Excepting the monobactams, metallo-β-lactamases can hydrolyze members of virtually every β-lactam class (*6*). Although the k_{cat} values for many of these substrates remain low (*6*, *7*), the selective pressures on catalytic optimization promise the emergence of higher activity metallo-β-lactamases, a process already in progress. The dinuclear metallo-β-lactamases are considered to be more highly evolved than their mononuclear counterparts and generally have higher k_{cat}/K_M values (*7*, *8*). Understanding the differences between the diverse metallo-β-lactamase family members and how they are adapting can lead to more efficient pharmaceutical design and can shed light onto the larger issue of evolution of antibiotic resistance mechanisms.

Serine-based β-lactamases are thought to be related to the bacterial transpeptidases (*9*). However, the origin of metallo-β-lactamase remains unclear, although an $\alpha\beta\beta\alpha$ structure suggests a gene duplication event (*10*), and structural homology to glyoxalase II has been noted, as well as sequence homology to several bacterial cyclase/dehydratases, aryl sulfatase, and PHNP (*11*−*13*). Refined crystal structures have been reported for four members of the metallo-β-lactamase family: the enzymes from *Bacteroides fragilis* (*14*), *Bacillus cereus* (*8*, *15*), *Stenotrophomonas maltophilia* (*16*), and *Pseudomonas aeruginosa* (*17*). These structures can be thought of as snapshots of a relatively young class of enzyme at different stages of maturation. In fact, allelic variants of several metallo-β-lactamases have been reported, further demonstrating the genetic diversity of this class (*18*−*21*). In particular, Fabiane et al. have suggested that the metallo-β-lactamase from *B. cereus*, originally characterized as a monozinc enzyme, is an evolutionary intermediate between the monozinc lactamases and the more active dizinc metallo-β-lactamases such as that from *B. fragilis* (*8*). This proposal is consistent with the different selective pressures placed on these two species in a clinical setting. *B. cereus* infections are usually associated with food poisoning for which antibiotics are not recommended, but members of the

† This work was supported in part by a National Institutes of Health grant (GM 56879-01) to S.J.B. and National Institutes of Health postdoctoral fellowships AI 10369 (W.F.) and GM 18061 (Z.W.).

* To whom correspondence should be addressed. Phone: (814) 865-2882. Fax: (814) 865-2973. E-mail: sjb1@psu.edu.

‡ Present address: Protein Science, Pharmacia Corporation, 7240-267-411, 301 Henrietta Street, Kalamazoo, MI 49007.

10.1021/bi001860v CCC: $20.00
Published on Web 01/17/2001

Scheme 1

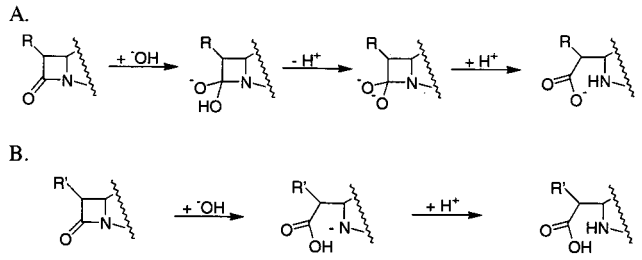

B. fragilis group can result in postsurgical infections and are avoided by prophylactic treatment with cephalosporins (*22*), which provides a driving force for optimizing enzyme activity.

Considerable mechanistic work on the metallo-β-lactamase enzyme from *B. cereus* has provided a kinetic and chemical mechanism in which C−N bond cleavage of cephalosporins (*23*) and benzyl penicillin (*24*, *25*) occurs at or after the rate-limiting step and requires protonation of the leaving lactam nitrogen (Scheme 1A). The more efficient dizinc lactamase from *B. fragilis* has overcome this kinetic barier: the C−N bond cleavage of nitrocefin (a chromogenic cephalosporin) occurs *before* the rate-limiting step and through a mechanism that, unlike the *B. cereus* mechanism, does not require protonation of the leaving lactam nitrogen before the bond is broken (Scheme 1B) (*26*). In fact, the C−N bond cleavage rate is about 375-fold higher than that of the *B. cereus* lactamase. These differences in rate and mechanism are somewhat surprising because the amino acid composition of the zinc ligands as well as other crucial active site residues remain identical, although the equivalents of bound zinc may vary depending on experimental conditions. Despite these similarities, clearly both structural and mechanistic differences exist between these two proteins. Determining which structural features are responsible for these improvements is of interest as these changes have resulted in a more efficient catalyst of antibiotic hydrolysis.

Although it is tempting to assign mechanistic differences as arising from specific features observed in the known structures, this method can be misleading because there is only 34% sequence identity between the two enzymes and significant differences are present both in the active site and throughout the protein. A more rigorous analysis can be conducted by grafting structural features of the various family members onto a common scaffold and evaluating the specific mechanistic consequences of each introduction. The two metallo-β-lactamase family members compared in this work are from *B. cereus* and *B. fragilis*. The specific features compared are position 104,[1] (Arg in *B. cereus* and Cys in *B. fragilis*) which lies beneath the dizinc center, and the presence (or absence) of a second equivalent of zinc bound at the active site. These two familial differences are explored within the framework of the *B. fragilis* enzyme to determine their effect on the kinetic sequence and aspects of the catalytic mechanism. This analysis bridges the structural and mechanistic data for these two lactamase enzymes and, in a broader sense, charts a small step in the evolution of multiple antibiotic resistance as conferred by the metallo-β-lactamases.

[1] The numbering used throughout is taken from ref *14*. To avoid confusion, residues from the *B. cereus* enzyme are numbered according to the structurally corresponding *B. fragilis* residue.

Table 1: Mutagenic Primers Used in This Study (5′ to 3′)

primer	sequence
C104R For	TGGCACGGCGATCGTATTGGCGGA
C104R Rev	TCCGCCAATACGATCGCCGTGCCA
*Nco*I For	CTGAGAGTGCACCCCATGGCACAGAAA
*Bam*HI Rev	GGAATACCGGGTAGGATCCTACAATTC

EXPERIMENTAL PROCEDURES

Materials. Except where noted, all chemicals were obtained through Sigma and all DNA modifying enzymes were purchased from New England Biolabs. Zn(II) and Co(II) standards were diluted from atomic absorption standard solutions into buffered solutions as described. Metallo-β-lactamase from *B. fragilis* was expressed and purified as described earlier (*27*). All buffers designated metal-free were prepared with milli Q water (Millipore) and treated with Chelex 100 (Bio-Rad Laboratories) according to the manufacturer's suggestions. Metal-free dialysis tubing was prepared as described earlier (*27*). Atomic absorption for Zn(II) content analysis was completed by using a Perkin-Elmer 730 atomic absorption spectrophotometer in the flame mode. Protein concentrations were determined by A_{280} using $\epsilon = 39\,000\ M^{-1}\ cm^{-1}$ (*27*). Routine UV−vis spectra and steady-state time courses were determined by using an OLIS/Cary 14 UV−vis spectrophotometer.

Construction, Expression, and Purification of C104R Lactamase. Overlap extension PCR[2] was used for construction of the C104R mutant (*28*). Briefly, the wild type *ccrA* gene on plasmid pMSZ01 (*27*) was used as a template for two separate PCR reactions, one using a *Nco*I For primer and a C104R Rev primer, and the other using a *Bam*HI Rev primer and a C104R For primer. All of the primers used were synthesized using an EXPEDITE nucleic acid synthesizer (PerSpective Biosystems, Inc., Framingham, MA) and are listed in Table 1. The products of these reactions were each pooled, precipitated and gel purified using a Qiaex II gel extraction kit (Qiagen). The resulting fragments were then combined along with *Nco*I For and *Bam*HI Rev primers for another round of PCR resulting in a full-length fragment (approximately 850 bp) containing the desired C104R mutation. This fragment and the expression vector pET-27b(+) (Novagen) were digested sequentially by *Nco*I and *Bam*HI; the PCR fragment and the 5.4 kb pET fragment were gel purified and ligated together using T4 DNA ligase (Promega) to create the kanamycin-resistant expression plasmid pWF02. This reaction mixture was electrotransformed into *Escherichia coli* DH5α cells (Life Technologies Inc.) and transformants selected with kanamycin. The exclusive presence of the desired mutation was verified by sequencing the entire lactamase gene from plasmid purified using a Midi purification kit (Qiagen). The pWF02 plasmid

[2] Abbreviations: ϵ, extinction coefficient; HEPES, *N*-[2-hydroxyethyl]piperazine-*N*′-2-ethanesulfonic acid; SDS−PAGE, sodium dodecyl sulfate−polyacrylamide gel electrophoresis; Tris, tris(hydroxymethyl)-aminomethane; Mes, 2-(*N*-morpholine)ethanesulfonic acid; UV−vis, ultraviolet−visible; V, steady-state rate of product formation; PAR, 4-(2-pyridylazo)resorcinol, TCEP, tris(2-carboxyethyl)phosphine; LMCT, ligand to metal charge transfer; PCR, polymerase chain reaction; bp, base pair; EXAFS, extended X-ray absorption fine structure; WT, wild-type.

was transformed into BL21(DE3) *E. coli* (Novagen) when used for expression and subsequent purification of the mutant protein via the same procedures as used for WT lactamase.

Extended Dialysis of WT Metallo-β-lactamase. In a sealed container, under a blanket of argon, WT lactamase (2 mL of 236 μM) was dialyzed against metal-free, argon-purged, pH 6.0 cacodylic acid (25 mM, 500 mL). Spectra/Por dialysis tubes (MWCO 10K) fitted with a screw cap (Spectrum) were used to facilitate removal of aliquots which were then diluted in dialysis buffer to 4−22 μM and stored at −70 °C before zinc quantification by atomic absorption. After each aliquot was taken, the dialysis buffer was changed and the argon blanket replaced. Samples were taken after 2, 4, 6, 8, 10, 12, 14, and 15 days of dialysis at 4 °C. Zinc content is described as a ratio of [zinc]/[protein].

Determining Zinc Content of Proteins Using PAR under Denaturing Conditions. Protein samples were diluted to a final concentration of 2−4 μM into freshly prepared metal-free 50 mM Hepes buffer, 4.52 M guanidine hydrochloride, 97 μM 4-(2-pyridylazo)resorcinol (PAR), pH 7.6. Zinc standards were prepared in concentrations ranging from 0 to 10 μM in the same buffer as described above. All samples were allowed to incubate at room-temperature overnight before A_{500} was measured. The zinc standards were fit to a linear plot and used to calculate the zinc concentrations of the protein samples which were expressed as [zinc]/[protein]. Addition of EDTA to the zinc standards resulted in an A_{500} close to the value predicted at 0 μM zinc, indicating that there is no metal contamination introduced by the PAR chelator.

Removing Zinc from WT or C104R under Native Conditions. In a 300 μL cuvette, 1 mM TCEP (Molecular Probes) and various concentrations of PAR (30, 150, 450, 750, 1050, and 1350 μM) in 50 mM metal-free Hepes, pH 7.6, were mixed with 3 μM of protein sample. The increase of A_{500} due to PAR_2Zn formation was observed for about 15 min until the reading stabilized. This value was compared with a zinc standard plot determined separately at each PAR concentration to determine the apparent zinc concentration of the protein sample under native conditions. This concentration was divided by the final protein concentration and subtracted from the total equivalent zinc bound value for each protein as determined by the denaturing experiments described above. The resulting values of equivalent zinc removed from the protein were plotted versus the [PAR]/[protein] ratios.

Batchwise Preparation of Zinc-Depleted Proteins. To prepare a larger quantity of zinc-depleted protein than for the spectrophotometric samples above, a batchwise process was used. Because TCEP complicates the kinetic measurements of WT lactamase (data not shown), all buffers were purged with argon immediately before use, and TCEP was omitted. For preparation of the WT zinc-depleted sample, protein (36.3 μM) was incubated with a 60-fold excess of PAR in MTEN buffer (50 mM Mes, 25 mM Tris, 25 mM ethanolamine, 100 mM NaCl) at pH 7.0 for 20 min at room temperature and subsequently spun through a 1.5 mL Sephadex G-25-150 gel filtration column preequilibrated with argon-purged, metal-free, MTEN buffer at pH 7.0. Protein concentration of the resulting solution was determined by A_{280} as before and the resulting preparation diluted as needed for other experiments. The monozinc C104R mutant was prepared in a similar manner by incubating protein samples (28 μM) for 20 min at room temperature with a 75-fold excess of PAR in argon-purged metal-free 50 mM Hepes, pH 7.6, followed by a spin column preequilibrated in the same buffer. If a different buffer was required for kinetic assays, the first spin column was followed by a second preequilibrated in the appropriate buffer. Denaturing PAR assays for zinc concentration showed no detrimental effect from adding a second spin column and verified the final [zinc]/[protein] value.

Cobalt Reconstitution of Zinc-Depleted C104R. Monozinc C104R mutant was prepared in metal-free 50 mM Hepes, pH 7.6 buffer as described above. The sample was divided into two aliquots (53.7 μM). To the first aliquot, 1.5 equiv of Zn(II) was added. To the second aliquot, 1.5 equiv of Co(II) was added. Both samples were incubated on ice for 0.5 h and the spectrum of each recorded. Because a slight amount of PAR (<0.05 equiv) was carried through the gel filtration column, a control reaction was included in which a comparable amount of PAR (2.85 μM) was incubated with the same concentrations of zinc or cobalt and the resulting spectra recorded. An extinction coefficient of $\epsilon_{340} = 820\ M^{-1}\ cm^{-1}$ (*27*) was used to quantify the observed Cys to cobalt ligand-to-metal charge-transfer (LMCT) band.

Steady-State Kinetics of β-Lactam Hydrolysis. Nitrocefin stocks were prepared fresh before each use; any particulate matter remaining in solution was removed by centrifugation. The concentration of stocks was determined using $\Delta\epsilon = 15\,900\ M^{-1}\ cm^{-1}$ for ΔA_{485} between intact and hydrolyzed nitrocefin (*29*). The rate of nitrocefin hydrolysis was determined at A_{485} for product formation from nanomolar concentrations of enzyme and 0−250 μM nitrocefin all in metal-free MTEN, pH 7.0 buffer. Measurements in D_2O were conducted in pD 7.0; MTEN and enzyme samples were exchanged into deuterated buffer by gel filtration. The rates of benzyl penicillin ($\Delta\epsilon_{235} = -775\ M^{-1}\ cm^{-1}$) and cephaloridine ($\Delta\epsilon_{265} = -6890\ M^{-1}\ cm^{-1}$) hydrolysis were determined using nanomolar concentrations of enzyme and 0−1 mM substrate all in metal-free MTEN pH 7.0 buffer. Steady-state parameters were derived using standard procedures.

Pre-Steady-State Kinetics of Nitrocefin Hydrolysis. Stopped-flow experiments were completed using MTEN, pH 7.0 buffer at 25° C that had been Chelex treated, argon purged, and subsequently degassed prior to use. To correct for the small amount of PAR carried through gel filtration columns used during preparation of zinc depleted proteins, these protein spectra were collected under the same experimental conditions as the hydrolysis reactions but without addition of substrate and were subtracted as background. A typical experiment rapidly mixed 5 μM lactamase with 20 μM nitrocefin using an Applied Photophysics SX.18mV stopped-flow spectrometer. Absorbance changes were measured at 390, 490, and 665 nm by using an absorbance photomultiplier or were measured from 300 to 725 nm by using an Applied Photophysics PD.1 photodiode array detector. Data from at least three reproducible experiments were averaged. Single wavelength stopped-flow absorbance data were converted to concentration data representing substrate, intermediate, and product as described earlier (*26*). These concentration data sets were simulated by the kinetic mechanism described later using the program Kinsim (C. Frieden and B. Barshop,

Table 2: Characterization of Lactamase Preparations

	WT[a]	PAR-treated WT	C104R	PAR-treated C104R
[Zn]/[protein]	2.0[b] ± 0.2	1.0[c] ± 0.2	2.3[b] ± 0.2	1.1[c] ± 0.2
$k_{cat(expt)}$ (s^{-1})	226 ± 6	101[d] ± 6	14.0 ± 0.7	4.2 ± 1.1
$K_{M(expt)}$ (μM)	7.1 ± 0.7	8.5 ± 1.5	5.0 ± 1.1	4.4 ± 0.7
k_{-1} (s^{-1})	4500	NA[e]	500	400
k_2 (s^{-1})	3700	NA	30	6.5
k_3 (s^{-1})	349	NA	150	150
$k_{cat(calcd)}$[f] (s^{-1})	309	NA	25	6.2
$K_{M(calcd)}$ (μM)	6.8	NA	4.4	3.9

[a] Values for WT lactamase were determined earlier (*26*). [b] Determined by atomic absorption. [c] Determined by the PAR assay for zinc under denaturing conditions. [d] Apparent k_{cat}; see text. [e] Not applicable; see text. [f] $k_{cat} = k_2k_3k_4/(k_2k_3 + k_2k_4 + k_3k_4)$; $K_M = (k_{-1} + k_2)k_{cat}/k_1k_2$.

Washington University, St. Louis, MO) (*30*, *31*) or KinTek-Sim (Kintek; http://www.kintek-corp.com).

RESULTS

Construction, Expression, and Purification of WT and C104R Lactamase. Using overlap extension PCR mutagenesis, the C104R mutant *B. fragilis* metallo-β-lactamase was prepared. Sequencing of the entire gene confirmed that this mutation was the only one introduced. Expression and purification of the protein was accomplished through the same procedure used for WT lactamase (*27*). Yields were generally slightly less for the C104R mutant (~7 mg/L culture) than those reported for WT (~20 mg/L culture), but this method still proved to be a high yield expression system for production of active, soluble, C104R mutant lactamase.

Determining the Total Zinc Content of C104R Using Atomic Absorption. After the last step of protein purification, a 72 h dialysis against metal-free buffer, the total zinc content of each protein sample was determined by atomic absorption. Zinc standards were used to construct a calibration curve, and the zinc concentration in each protein sample was determined by the average of triplicate measurements. Residual zinc content in the final dialysis buffer was negligible compared to the protein. The C104R mutant was determined to harbor 2.0 ± 0.3 equiv of zinc/monomer of protein (Table 2).

Extended Dialysis of WT Metallo-β-lactamase. In an attempt to remove 1 equiv of zinc from WT lactamase, the protein was dialyzed at pH 6.0 for 15 days. Aliquots were removed periodically for quantification of zinc content by atomic absorption and protein concentration by A_{280}. Although previous investigators have reported a gradual loss of 1 equiv of Zn over a comparable dialysis period, we observed only a slight decrease (<0.3 equiv) in measured [Zn]/[protein] ratios (Figure S1; Supporting Information) (*32*).

Determining the Total Zinc Content of Proteins Using PAR. The colorimetric zinc chelator 4-(2-pyridylazo)resorcinol (PAR) was used to measure the total zinc concentration of the proteins studied by incubating the PAR and protein under denaturing conditions. The absorbance at 500 nm as compared to a series of zinc:PAR standards was used to calculate the concentration of total zinc in the sample. The error in zinc concentration determinations by PAR is estimated at approximately 13% (*33*). The zinc concentrations determined were divided by protein concentrations to give the equivalents of zinc per protein molecule and are presented in Table 2. Values for the dizinc proteins WT and C104R matched within error the values determined by atomic absorption (data not shown).

Removing Zn from WT or C104R Lactamase under Native Conditions. To remove various amounts of metal from dizinc WT and dizinc C104R lactamase under native conditions (*34*), PAR was incubated with the enzyme at various PAR:protein ratios. The increase in absorbance at 500 nm was used to calculate the amount of zinc chelated by PAR and therefore removed from the protein. This value was subtracted from the total zinc concentration of the protein based on denatured samples and plotted against the PAR:protein ratio as shown in Supporting Information. The WT lactamase lost about 0.9 equiv at low PAR:protein ratios; the zinc remaining bound to the protein could be totally removed upon increasing the PAR concentration. The C104R mutant behaved somewhat differently. Upon increasing the PAR concentration, the equivalent of Zn remaining bound to the protein leveled off at around 0.7 equiv remaining and was refractory to further increases in the PAR concentration.

Removing 1 Equiv of Zn from WT or C104R, Batchwise Preparation. To prepare larger amounts of 1-equiv-zinc proteins, each protein was incubated with PAR under native conditions and then subjected to two sequential spin columns to remove the excess PAR, any unbound zinc, and to exchange buffer systems if necessary. Although most of the PAR was removed, a small amount, approximately 0.05 equiv as measured by absorbance at 400 and 500 nm, could not be removed by gel filtration. Although this contaminant complicated some spectra, it could be subtracted as background and was not expected to influence the kinetics significantly. To confirm the expected zinc:protein ratios, these PAR-treated samples were subsequently subjected to the denaturing PAR assay for total zinc content as described above and the results are shown in Table 2.

Cobalt Reconstitution of Zinc-Depleted C104R Lactamase. C104R lactamase containing approximately 1 equiv of zinc was prepared as described above. This sample was divided into two aliquots. To one sample, 1.5 equiv of Co(II) was added; to the other, 1.5 equiv of Zn(II) was added and their UV−vis absorbance spectra compared as shown in Figure S3 (Supporting Information). The sample with added Co(II) showed an increase in absorbance at 340 nm relative to the Zn(II) sample. On the basis of an expected Cys to Co(II) LMCT [$\epsilon_{340} = 820\ M^{-1}cm^{-1}$ (*22*)], this band accounted for 52 μM enzyme which compares favorably with the 53.7 μM concentration of protein used for the spectroscopy.

Steady-State Kinetics of Nitrocefin Hydrolysis. Steady-state parameters for dizinc WT (*22*), dizinc C104R, 1-equiv-zinc

Table 3: Hydrolysis of Other β-Lactam Substrates

	benzyl penicillin		cephaloridine	
	k_{cat} (s^{-1})	K_M (μM)	k_{cat} (s^{-1})	K_M (μM)
WT[a]	142 ± 4	19 ± 2	74 ± 2	5 ± 4
C104R	36 ± 2	34 ± 6	44 ± 3	42 ± 8
PAR-treated C104R	10 ± 1	22 ± 8	28 ± 3	42 ± 10

[a] Enzyme samples were prepared as described for Table 2.

WT, and monozinc C104R lactamases were determined (Table 2). Dizinc C104R has a K_M value slightly lower than dizinc WT. The k_{cat} value was significantly decreased by about 16-fold. When the dizinc and monozinc proteins are compared, little change in K_M is observed upon removal of one zinc. The k_{cat} for 1-equiv-zinc WT is about 45% of that determined for dizinc WT. The k_{cat} for monozinc C104R is about 30% of that determined for dizinc C104R. The k_{cat} values for zinc-depleted proteins were not reproducible unless samples were prepared and measured in buffer that was purged with argon prior to the manipulations. The k_{cat} and K_M values for monozinc C104R were also determined in buffered D_2O containing MTEN pD 7.0 as 2.9 ± 0.1 s^{-1} and 4.4 ± 0.8 μM, respectively, giving a $k_{cat}^{H_2O}/k_{cat}^{D_2O}$ ratio of 1.4 ± 0.4. Hydrolysis of other representative β-lactams, benzyl penicillin and cephaloridine, also shows a decrease in both k_{cat} and k_{cat}/K_M values upon C104R mutation and removal of the second equivalent of zinc (Table 3).

Pre-Steady-State Kinetics of Nitrocefin Hydrolysis. Diode-array stopped-flow experiments using the enzyme preparations described above were compared with those collected earlier for WT metallo-β-lactamase (*26*). The dizinc C104R mutant mixed with nitrocefin showed absorbance peaks for substrate at 390 nm, product at 490 nm and intermediate at 665 nm. Although the accumulation of the 665 nm peak is significantly decreased from that observed with the WT enzyme (Figure 2A), the presence of this peak is indicative of the same anionic intermediate. Reaction of nitrocefin with the monozinc C104R mutant showed absorbance peaks for substrate and product, but only a very minor absorbance peak is visible at 665 nm for the intermediate (Figure 3A).

Single-wavelength stopped-flow spectroscopy for each enzyme preparation was collected and compared with that determined earlier for WT lactamase (*26*). Because of the appearance of an absorbance peak at 665 nm in nitrocefin hydrolysis reactions by each of the enzyme preparations, all of the single-wavelength data were fit to the same minimal kinetic mechanism as WT, a linear mechanism with one obligatory spectral intermediate (Scheme 2). This model gave acceptable fits for all experiments. For all simulations, the constants k_1 and k_{-4} were fixed at diffusion limits and product release was set at a lower limit of 10^4 s^{-1} (*26*). As noted before, k_{-1} and k_2 can be varied over a wide range and still provide reasonable fits if they are varied as a pair (*26*). These constants were constrained to values that result in calculated steady-state parameters, k_{cat} and K_M, consistent with experimentally measured values (Table 2).

The time-dependent concentration traces for hydrolysis of nitrocefin by the WT lactamase containing 1 equiv of zinc were fit to the same kinetic mechanism as WT; a linear mechanism with decay of the intermediate as the rate-limiting step. Because steady-state data suggested that hydrolysis may be due to half of the enzyme preparation containing two zinc ions per protein monomer and half being apoprotein (see below), simulations were preformed using the microscopic constants determined for WT enzyme, but halving the actual enzyme concentrations for the simulations. This produced reasonable fits to the observed data as shown in Figure 1. The concentration data for nitrocefin hydrolysis by the dizinc C104R mutant were also well fit using the same kinetic mechanism, although k_{-1}, k_2, and k_3 values were all slower than those determined for WT lactamase, and with the ratio of k_2:k_3 shifted so that k_2 was now the slowest step in the reaction. However, k_2 was less than 10-fold slower than k_3 so the intermediate was still easily observable during the experimental time frame (Figure 2B, Table 2). The data for nitrocefin hydrolysis by the monozinc C104R mutant also were fit satisfactorily by the same kinetic mechanism (Figure 3B, Table 2). Simulations using the kinetic constants for dizinc C104R with the enzyme concentration set at half of its actual concentration did not describe the observed data (Figure 3B, dotted line). Introduction of a minor adjustment in k_{-1}, coupled with a more significant 5-fold decrease in k_2, provided fits to the observed data (Table 2, Figure 3B, solid line) using the experimental enzyme concentration determined by A_{280}. Although less intermediate accumulated than with the dizinc C104R mutant, the k_3 step still followed the same decay rate. As shown in Table 2, the values for the steady-state parameters calculated from individual rate constants for each enzyme preparation match reasonably well with experimentally derived values.

Scheme 2

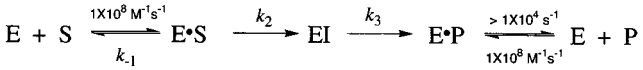

DISCUSSION

The metallo-β-lactamase family is a diverse collection of enzymes evolving under considerable selective pressures. A low-activity enzyme isolated from *B. cereus* tightly binds 1 equiv of zinc and has relatively slow k_{cat} values for lactam hydrolysis as compared with other lactamases (*6*). The rate-limiting step has been reported as preceding or concomitant with C−N bond cleavage (*23*−*25*). This enzyme can weakly bind a second equivalent of zinc, resulting in a modest 2-fold increase in k_{cat} values (*35*). This ability to bind either 1 or 2 (albeit weakly) equiv of zinc suggests that this protein may be an evolutionary intermediate between the monozinc β-lactamases and the more active dinuclear zinc β-lactamases such as the enzyme isolated from the more threatening pathogen *B. fragilis* (*8*). The dinuclear lactamase from *B. fragilis* shares 34% sequence identity with the *B. cereus* enzyme as well as retaining identical primary zinc ligands, but there are differences observed in the affinity for zinc and in the amino acid composition of the active site flap, of residues surrounding the primary zinc ligands, and throughout the entire protein. Unlike the *B. cereus* lactamase, this enzyme tightly binds 2 equiv of zinc rather than 1 and has k_{cat}/K_M values generally increased by 10-fold (*7*). Most notably, selective pressures on this enzyme have resulted in acceleration of the slowest catalytic step. In the case of nitrocefin hydrolysis, the C−N bond cleavage rate is accelerated by 375-fold so that it is no longer rate limiting in the *B. fragilis* mechanism. The slowest step in *B. fragilis*

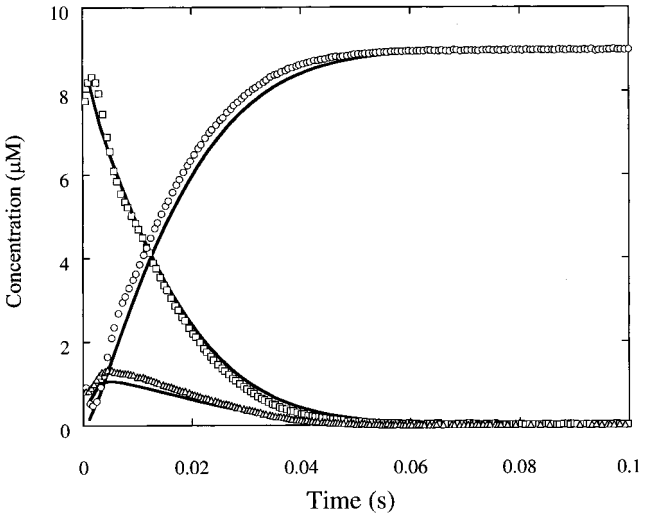

FIGURE 1: Time course for nitrocefin hydrolysis by 1-equiv-zinc WT metallo-β-lactamase. Protein (5 μM) was rapidly mixed with 9 μM nitrocefin in MTEN pH 7.0 at 25° C. The concentration of substrate (squares), intermediate (triangles), and product (circles) were calculated from absorbance traces at 390, 665, and 490 nm as described in Experimental Procedures. Simulated progress curves are shown in solid lines and are derived from the values for dizinc WT lactamase in Table 2 and Scheme 2 except that the enzyme concentration is set to 2.5 μM in the simulations.

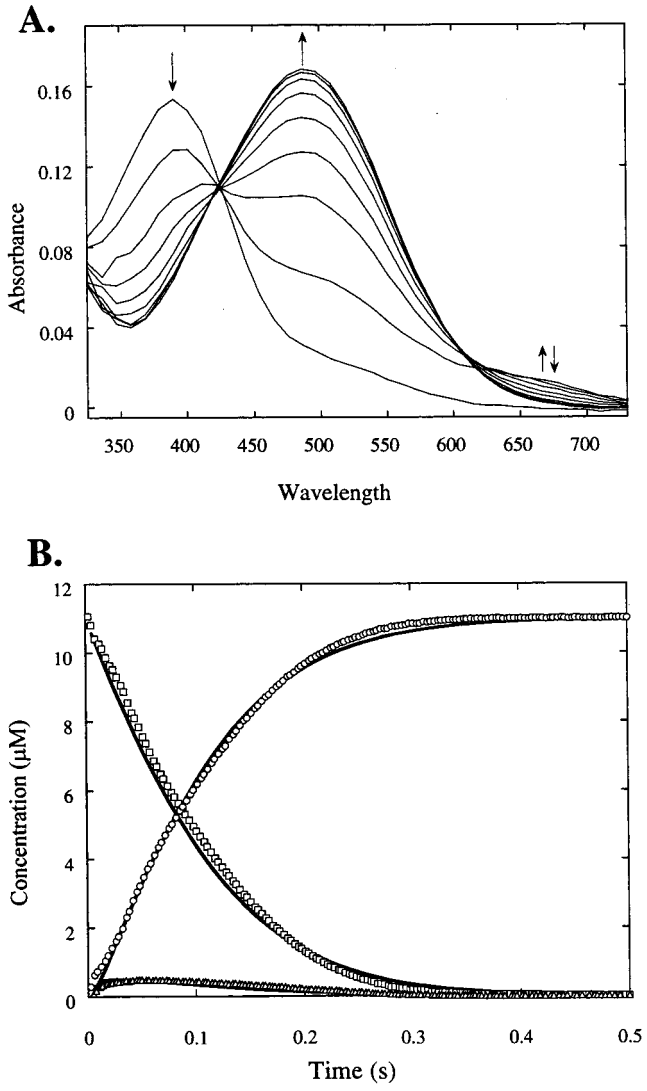

FIGURE 2: Stopped-flow spectroscopy of dizinc C104R metallo-β-lactamase. Protein (5 μM) was mixed rapidly with nitrocefin (11 μM) in pH 7.0 MTEN at 25° C. (A) Absorbance spectra from 325 to 725 nm are recorded 1.28 ms after mixing and every 40 ms thereafter. The reaction was complete after 340 ms. Absorbance values decrease at 390 nm, increase at 490 nm, and decrease after an initial rise at 665 nm. (B) Concentrations for substrate (squares), intermediate (triangles), and product (circles) were calculated as described in Experimental Procedures. Simulated cures are shown in solid lines and are derived from the values in Table 2 and Scheme 2.

mediated hydrolysis has been identified as protonation of an anionic C−N bond cleaved intermediate (Scheme 1B) (*26*, *27*). This rate acceleration results in more efficient inactivation of antibiotics. Therefore, it is of considerable interest to understand how nature continues to improve the catalytic mechanism of these enzymes specifically by overcoming the kinetic hurdle of a slow C−N bond cleavage rate.

Toward these ends, we have evaluated the mechanistic consequences of structural differences that have evolved between the *B. cereus* and *B. fragilis* metallo-β-lactamase enzymes through kinetic studies of several forms of the *B. fragilis* enzyme: a mutant in which the cysteine 104 is replaced by the arginine found in *B. cereus*, and *B. fragilis* proteins (WT and C104R) containing only 1 equiv of bound zinc. These changes mimic a key structural feature and the metal ion composition found in the *B. cereus* enzyme and probe whether they can account for the observed differences in rate-limiting step and zinc stoichiometry.

WT Lactamase with 1 Equiv of Bound Zinc. Recent model studies have suggested that a dinuclear active site does not confer much advantage over a mononuclear site (*36*, *37*). To quantify these differences in an enzyme system, we prepared a monozinc WT lactamase from *B. fragilis*. Paul-Soto et al. have generated the monozinc WT protein and reported a k_{cat} value for nitrocefin hydrolysis only 20% less than that of the dizinc form and a K_M value that is virtually unchanged (*32*). Steady-state kinetic parameters, however, can often mask changes in rate-determining steps, so we attempted to revisit the kinetics of the monozinc WT enzyme with a more detailed analysis. To probe the contribution specifically of Zn2 to the dizinc active site of the WT enzyme, efforts were made to remove this metal either by extended dialysis or by mutations of the Zn2 ligands and surrounding residues. In our hands, extended dialysis of the WT protein did not remove a significant amount of zinc from the protein (Figure S1).

By treating the WT lactamase with a colorimetric zinc chelator under native conditions, we were able to successfully remove 1 equiv of zinc from the protein. Steady-state parameters, however, showed an unchanged K_M value and a k_{cat} value that was reduced to approximately half of the WT value. These results immediately suggested the possibilities that either all of the enzyme had one zinc ion bound or half of the enzyme had two zinc ions bound and the other half was inactive apoprotein. Pre-steady-state kinetics of nitrocefin hydrolysis confirmed the latter; using the identical kinetic mechanism and rate constants determined for the dizinc WT lactamase, the experimental traces for the 1-equiv-zinc WT lactamase could be reasonably approximated by reducing the enzyme concentration in the simulation by 50%.

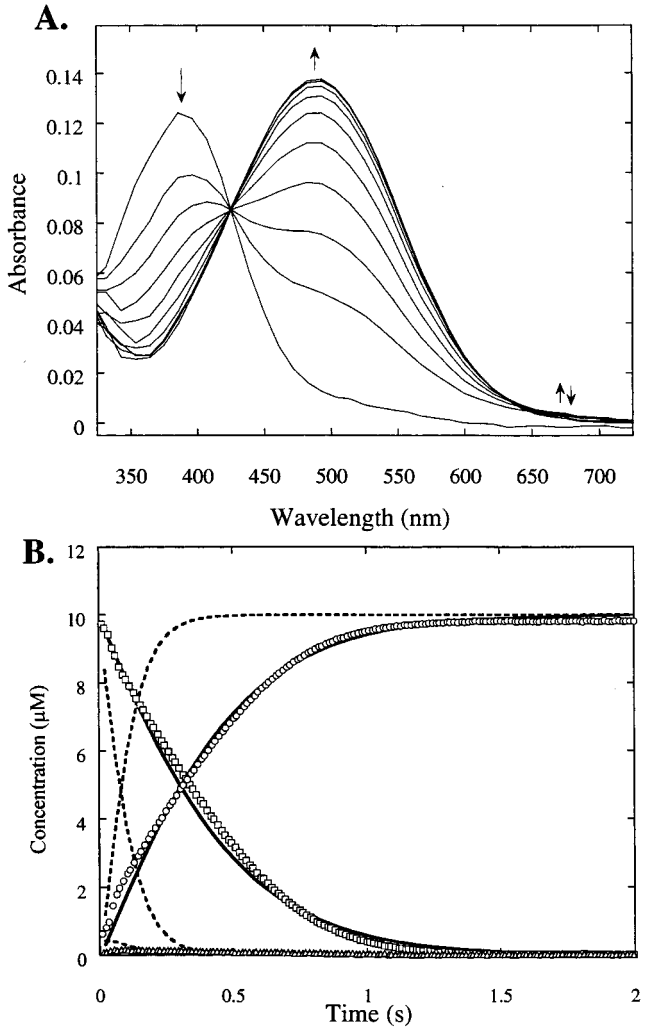

FIGURE 3: Stopped-flow spectroscopy of monozinc C104R metallo-β-lactamase. Protein (5 μM) was rapidly mixed with nitrocefin (10 μM) in pH 7.0 MTEN at 25° C. (A) Absorbance spectra from 325 to 725 nm were recorded 1.28 ms after mixing and every 128 ms thereafter. The reaction was complete after 1.153 s. Absrobance values decreased at 390 nm, increased at 490 nm, and decreased after a small increase at 665 nm. (B) Concentrations for substrate (squares), intermediate (triangles), and product (circles) were calculated as described in the Experimental Procedures. Curves are simulated acording to Scheme 2 using an enzyme concentration of 5 μM and the kinetic constants for monozinc C104R in Table 2 (solid lines) or with an enzyme concentration set at 2.5 μM and the kinetic constants for dizinc C104R lactamase from Table 2 (dashed line).

In our hands, the monozinc WT metallo-β-lactamase does not appear to be stable under dilute conditions and suggests that a cooperative binding of Zn2 may contribute to stability of the holoenzyme.

Two single mutants (C181S and H223A) and one double mutant (C181S and C104R) all resulted in proteins that precipitated upon purification (data not shown), suggesting that the Zn2 may play a necessary structural role in soluble expression of the *B. fragilis* isoform and that mutation of the Zn2 ligands gives rise to an unstable protein. Although Li et al. have reported the structure of a monozinc C181S mutant, this protein was also refolded from inclusion bodies and crystallized under high protein concentrations (*38*). The significant loss in activity attributed to the Cys to Ser mutation (*38*, *39*) may arise from the instability of the monozinc form under dilute conditions where steady-state kinetic assays are usually performed. Although not a direct Zn2 ligand, one of the residues closely bordering the active site in the monozinc *B. cereus* enzyme is Arg 104, whose positive charge has been proposed to destabilize Zn2 binding (*8*). We found that the *B. fragilis* C104R single mutation resulted in a dizinc and not a monozinc protein as predicted, a result recently confirmed by Yang et al. (*39*). In summary, our attempts at dialysis and mutagenesis were unsuccessful in preparing a WT monozinc lactamase.

Dizinc C104R Single Mutant. In the structure of the dizinc *B. cereus* enzyme, the guanidino nitrogens of Arg104 are within hydrogen-bonding distance of Asp103, a direct ligand to the weakly bound Zn2 ion, and to the backbone carbonyl oxygens of Gly222 and Asn55 (Figure 4) (*8*, *14*, *15*). The residues Asp103, Gly222, and Asn55 are conserved in *B. fragilis* so it was hypothesized that introduction of Arg at position 104 would approximate the structure found in *B. cereus* and destabilize Zn2 either by electrostatic repulsion or by repositioning some of the Zn2 ligands. The three histidine ligands of the tightly bound Zn1 are structurally very similar in the *B. cereus* and *B. fragilis* enzymes and are not expected to be significantly changed by the C104R mutation. As discussed above, this mutation did not recreate a monozinc protein but did have a significant effect on k_{cat}, decreasing the value from 226 to 14 s^{-1}, and approximately reproducing the value measured for the dizinc *B. cereus* enzyme, 12 s^{-1}.[3]

Pre-steady-state measurements on the dizinc C104R mutant revealed more about its mechanism of action. Transient kinetic analysis of the dizinc *B. cereus* enzyme has not yet been reported, but results of the dizinc C104R mutant can be compared to its WT parent. During nitrocefin hydrolysis, transient formation of an intermediate with a spectrum that centered at 665 nm was observed. This is the same spectral species observed during hydrolysis by the *B. fragilis* WT lactamase, suggesting that the dizinc C104R mutant proceeds through the same chemical mechanism as WT by expelling the leaving lactam nitrogen as an anion. The amount of intermediate accumulated, however, was less than that observed with WT lactamase. The pre-steady-state substrate, product, and intermediate concentration traces could be fit by using the same minimal kinetic mechanism as described for the WT lactamase, a linear mechanism with one obligatory intermediate (Scheme 2). The rate constants determined for the fit, however, were much different, revealing a lower K_d value for nitrocefin due to a decreased k_{-1} and a k_{cat} value that is determined mostly by k_2 rather than k_3. The most drastic decrease in rate is observed for k_2 which proceeds more than 120-fold slower than the same step in WT lactamase. The rate of k_3 is also slowed, but only by about 0.5-fold, changing the ratio of k_2 and k_3 to favor k_2 as the major factor in determining k_{cat} values. Although the same anionic intermediate as seen with WT enzyme is still observed during hydrolysis by the C104R mutant, introduction of the second-shell C104R mutation has changed the magnitude of k_{cat} and the identity of the rate-

[3] Steady-state parameters for the *B. cereus* wild-type metallo-β-lactamase were measured in MTEN, pH 7.0, buffer with <100 nM Zn(II) for the monozinc form of the enzyme and at 1.5 mM Zn(II) for the dizinc form of the enzyme.

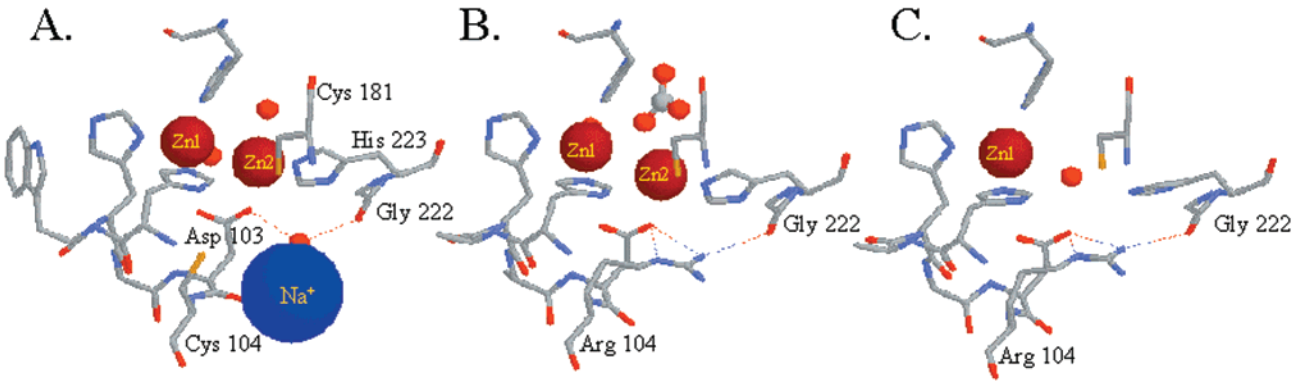

FIGURE 4: Active-site structures of metallo-β-lactamase family members. (A) Taken from 1ZNB, the active site of dizinc *B. fragilis* lactamase shows a Zn−Zn distance of 3.46 Å, a bridging water and a Cys 104 residue distant from the Zn2 site. Small red spheres are ordered water molecules. (B) Taken from 1BVT, the active site of dizinc *B. cereus* lactamase with bound bicarbonate shows a longer Zn−Zn distance of 3.81 Å and Arg 104, a second shell Zn2 ligand. (C) Taken from 1BMC, the active site of monozinc *B. cereus* lactamase shows a similar configuration of Arg 104, but Zn2 is replaced by an ordered water molecule. The view of all of the sites shown is from the inside of the protein looking outward; substrate is expected to bind behind the structures as drawn.

limiting step to approximate that of the dizinc *B. cereus* lactamase.

Monozinc C104R Lactamase. Attempts to prepare a monozinc C104R protein were more successful than with WT enzyme. Incubation under native conditions with varying amounts of the zinc chelator PAR led to the facile removal of 1 equiv of zinc, but then became refractory to further zinc removal when approximately 0.7 equiv of zinc remained bound to the mutant. This observation was different than that observed for WT where increasing the chelator concentration could pull both zinc ions out of the protein, suggesting that the cooperative nature of the dizinc binding site may be disrupted by this mutation. Addition of cobalt(II) to the monozinc C104R species resulted in the appearance of a LMCT band at 340 nm, consistent with assigning the empty zinc site as the Cys181-containing Zn2 site.

It should be noted that while the assignment of the monozinc binding site as Zn1 is the most likely option based on structural analogy and the appearance of a Co(II)−Cys LMCT band upon addition of cobalt to the monozinc enzyme, the existence of a monozinc mutant with the metal in the Zn2 site should not be entirely ruled out. Cadmium has been shown to have an intrinsic affinity for the Zn2 site of the *B. cereus* enzyme (*40*). If cobalt also has a preference to bind at the Zn2 site, equilibration after addition of cobalt to the monozinc protein may make interpretation of the observed LMCT band problematic. Also, a similar complex is thought to occur during nonenzymatic hydrolysis of benzylpenicillin by Cu(II) ions (*41*), and there is some evidence for an active monozinc β-lactamase from *Aeromonas hydrophilia* which has only Zn2 bound (*35*). Although assigning monozinc binding at the Zn1 site is preferred, definitive characterization of zinc binding to mono- and dizinc C104R will have to wait for completion of EXAFS studies currently underway.

Steady-state parameters for nitrocefin hydrolysis by this monozinc mutant showed little or no change in K_M (as compared to the dizinc mutant), but k_{cat} was decreased by about 70% to 4.4 s^{-1}, approximating the k_{cat} of the monozinc *B. cereus* enzyme, 6 s^{-1}.[3] The K_M values for both the mono- and dizinc enzymes remain lower than those typically reported for nitrocefin hydrolysis by *B. cereus* (*7*, *42*), probably due to the differences remaining in the active site and flap residues shown to be important in binding substrate and inhibitor (*43*, *44*). The kinetic solvent isotope effect on k_{cat} for nitrocefin hydrolysis by the monozinc C104R mutant drops significantly from the WT value of (H/D) 2.5 ± 0.1 to that of (H/D) 1.4 ± 0.4, approximating the value reported for hydrolysis of cephaloridine by the *B. cereus* enzyme, (H/D) 1.5 ± 0.5 (*25*). At low pH values, the pH rate profiles for the monozinc *B. cereus* enzyme indicated the requirement of two basic residues for catalysis, a feature not reproduced with the monozinc C104R mutant as the pH vs k_{cat} profile remains relatively flat at values where the protein is stable (data not shown). Removing Zn2 from the C104R mutant reproduces several features observed with the monozinc *B. cereus* lactamase including the magnitude of k_{cat} and the solvent isotope effect on k_{cat}.

A pre-steady-state analysis reveals more about the mechanism of this monozinc mutant. Spectra recorded during pre-steady-state kinetics of monozinc C104R showed a significant reduction in the buildup of the 665 nm spectral intermediate, although a small amount was still observable, and also did not suggest the presence of any other spectral species (Figure 3). When the concentration traces of substrate, product, and intermediate were simulated by using the rate constants for dizinc C104R, but with the enzyme concentration decreased by 50% of that used in the actual experiment, the traces did not fit the experimental data, suggesting that hydrolysis was not occurring by half of the C104R enzyme with both zinc ions bound as was found to be the case with 1 equiv of zinc WT lactamase. Instead, the more likely interpretation is that the majority of the enzyme contains a single zinc ion, with resulting changes in both k_{cat} and K_M and some rate constants for individual steps.

Data fitting required a reduction of k_2 and a slight decrease in k_{-1} in the kinetic simulations in order to obtain reasonable fits using the true experimental enzyme concentration. The decay of the intermediate could be fit to the same rate constant as the dizinc mutant, suggesting that monozinc C104R also can proceed through the same mechanism as the dizinc form but that k_2 is now much more limiting.

Earlier authors have assigned the microscopic rate constants for nitrocefin hydrolysis by the monozinc *B. cereus* metallo-β-lactamase under cryoenzymological conditions (*23*, *45*). A branched pathway was determined that included a

distinct spectral intermediate on the slower branch that was attributed to a noncovalent intermediate with an intact C−N bond. This intermediate, however, was only observed at temperatures less than −54 °C. In fact, an extrapolation of Arrhenius plots for the microscopic rate constants suggests that the slower branch becomes less significant and may disappear at room temperature [in contrast to the Arrhenius plots for hydrolysis of benzyl-penicillin by the Co(II) *B. cereus* lactamase in which a branched pathway is still predicted (*23*) and observed (*24*) at room temperature]. No evidence has been presented at any temperature in the *B. cereus* case for an N-deprotonated intermediate as is seen in the *B. fragilis* WT mechanism or in the other enzyme preparations reported here. Removal of Zn2 from the C104R mutant does not result in a branched pathway. This may be a consequence of either the remaining structural differences between these two family members or a result of collecting the pre-steady-state data at room temperature under aqueous conditions. Removing Zn2, however, does further shift the ratio of k_2:k_3 resulting in a k_2 (assigned as C−N bond cleavage) that almost exclusively regulates k_{cat}. The monozinc C104R mutant approximates many of the mechanistic features of the monozinc *B. cereus* enzyme, specifically the magnitude of and solvent isotope effect on k_{cat} values as well as the regulation of k_{cat} by a slow C−N bond cleavage rate. In sum, introducing C104R into the *B. fragilis* lactamase and subsequent removal of Zn2 is sufficient to mimic many of the mechanistic features observed in the *B. cereus* mono- and dizinc metallo-β-lactamase.

Role of Position 104 and the Cocatalytic Zinc Site. The amino acid residue located at position 104 is variable within the metallo-β-lactamase family. In addition to the arginine and cysteine residues discussed above, serine or a Zn2-ligating histidine also occupy this position in β-lactamases from other species (*46*). However, all of the naturally occurring lactamase enzymes known to bind stably 1 equiv of Zn(II) have arginine in this position, suggesting that this residue is important in either forming or stabilizing the monozinc form of the protein. The C104R mutant is isolated as a dizinc protein, but is also stable as a monozinc preparation in contrast to the WT protein, indicating that Arg104 is not sufficient to eliminate Zn2 binding, but may be necessary to help stabilize the monozinc form. Characterization of zinc stoichiometry in other lactamase family members will be required to determine the generality of this observation.

The residue at position 104 also has a significant effect on the magnitude of the microscopic rate constants and the identity of the overall rate-determining step of nitrocefin hydrolysis. The C104R mutation results in tighter ground-state binding of both ES (1.3 kcal/mol) and EI (0.5 kcal/mol), although the differences in stabilization suggest that the interaction of this group with each intermediate vary in importance. The magnitude of the ground-state effect is similar to that observed by other authors for second shell mutations (*47*). The importance of electrostatics in the active site and surrounding protein to reaction pathways in β-lactamase mechanisms has been calculated (*48*, *49*). As observed here, binding of the negatively charged substrate and intermediate complexes to lactamase is enhanced by inserting a positive charge into the ligand field. The $ES^{\ddagger}$, however, does not appear to be stabilized, but destabilized by about 2.8 kcal/mol. While a decrease in hydroxide reactivity is expected upon introduction of a nearby positive charge, the magnitude of the observed effect is larger than might be expected for a second shell zinc ligand (*47*). Small structural perturbations of the dinuclear active site may also be partially responsible for the decrease in reaction rate and will have to await further characterization for their evaluation.

Removal of 1 equiv of zinc from the C104R mutant results in a slight stabilization of the ES complex over that of the dizinc form, but has its most significant effect in further destabilizing $ES^{\ddagger}$ by 0.9 kcal/mol. This result demonstrates the true cocatalytic nature of the dinuclear zinc active site, showing that each zinc does in fact contribute to the catalysis of C−N bond cleavage. This drop in rate is not due to a decrease in the concentration of zinc-hydroxide as the pH rate profile of k_{cat} remains relatively flat near pH 7.0 for the monozinc C104R mutant (data not shown). The decay rate for monozinc EI can be fit to the same constant determined for the dizinc form, therefore presence of two equiv of zinc does not seem to be necessary for stabilization of the N-deprotonated intermediate. The reduction in k_2 upon formation of the monozinc enzyme probably results from both the loss of amide bond polarization and of stabilization of the tetrahedral adduct formed after hydroxide attack, similar to that proposed in the dinuclear *Aeromonas* aminopeptidase mechanism (*50*).

The catalytic advantages of Cys 104 and a dinuclear zinc center are also reflected in hydrolysis of more clinically relevant β-lactams such as benzyl penicillin and cephaloridine, each showing significant increases of both k_{cat} and k_{cat}/K_M values (Table 3). While the electron-withdrawing dinitrostyrene moiety of nitrocefin may help in stabilizing an anionic intermediate, benzyl penicillin and cephaloridine do not contain this substitutent. The pK_a of the ring nitrogen in hydrolysis products of these lactams is estimated to be at least 11 units higher than that of nitrocefin, suggesting that protonation may be required for C−N cleavage of these substrates. Relating the steady-state hydrolysis rates of these compounds to changes in the protein structure is problematic because their kinetic mechanisms and the nature of their rate-limiting steps remain undefined. Regardless, the differences in steady-state hydrolysis rates for these compounds indicate a possible survival advantage of bacteria expressing similar metallo-β-lactamases when challenged with a clinically relevant β-lactam.

Family of Metallo-β-Lactamases. Taken together, the identity of the residue at position 104 and the presence of Zn2 appear to be two structural features necessary for the accelerated C−N bond cleavage rate for nitrocefin seen in the *B. fragilis* metallo-β-lactamase over that of the *B. cereus* lactamase. If the directionality of these evolving familial differences is assigned according to increasing enzyme activity and more stringent selective pressures likely encountered in a clinical setting, a tentative scheme for the evolution of this catalytic mechanism can be proposed. An ancestral monozinc Arg104-containing enzyme may start with significant β-lactamase activity but would have a slow, rate-limiting C−N bond cleavage rate. Selective pressures on this low k_{cat} could lead to subtle structural variations that allow for tighter binding of a second zinc equivalent, accelerating C−N bond cleavage. Upon binding of both zincs, Arg104 is no longer required for protein stability and

would be allowed to mutate. Removal of this positive charge by mutation destabilizes ES and EI as well as accelerates the C−N bond cleavage rate, probably due to electrostatics and a subtle reorganization of the dinuclear site, resulting in a dinuclear enzyme that has overcome the kinetic hurdle of a slow C−N bond cleavage rate. In the case of the *B. fragilis* lactamase, mutation of 104 and addition of a second equivalent of zinc provide 3.7 kcal/mol toward acceleration of C−N bond cleavage although some of this effect is masked in the steady-state rate by a change in rate-limiting step. The dinuclear WT hydrolysis rate is an order of magnitude greater than the monozinc mutant rate and mirrors the same trend observed in other naturally occurring metallo-β-lactamase enzymes (*7*). It should be noted that the different Zn2 ligands found in the dinuclear metallo-β-lactamase from *Stenotrophomonas maltophilia* demonstrate an alternative solution that also increases C−N bond cleavage rates (*51*). By introducing mutations found in naturally occurring metallo-β-lactamase variants into a common framework, progress has been made toward understanding the structural basis behind the mechanistic differences found in this family of enzymes and is illustrative of one small step in the evolution of multiple antibiotic resistance mechanisms.

CONCLUSION

Contributions of each zinc ion and the residues surrounding the dinuclear active site of metallo-β-lactamase from *B. fragilis* are probed using site-directed mutagenesis and a metal chelator. Mutation of a second shell residue influences hydrolysis rates of nitrocefin by perturbing substrate binding and C−N bond cleavage rates. Both zinc ions are also shown to contribute toward catalysis of C−N bond cleavage, demonstrating the cocatalytic nature of the dinuclear active site. These changes occur in natural variants of metallo-β-lactamase and chart one step in the optimization of the catalytic mechanism.

ACKNOWLEDGMENT

We are grateful to Dr. Alejandro J. Vila and Fito Rasia for the kind gift of WT *B. cereus* metallo-β-lactamase, and Dr. Henry Gong for assistance with atomic absorbance measurements. We also thank Dr. Ann M. Valentine for helpful discussions and a thorough reading of this manuscript.

SUPPORTING INFORMATION AVAILABLE

Zinc quantification of dialyzed WT lactamase, zinc content of PAR treated WT, and C104R lactamases, and spectra of zinc and cobalt substituted C104R lactamase. This material is available free of charge via the Internet at http://pubs.acs.org.

REFERENCES

1. Levy, S. B. (1992) *The Antibiotic Paradox: How miracle drugs are destroying the miracle*, Plenum Press, New York.
2. Medeiros, A. A. (1997) *Clin. Infect. Dis. 24* (Suppl. 1), S19−S45.
3. Fey, P. D., Safranek, T. J., Rupp, M. E., Dunne, E. F., Ribot, E., Iwen, P. C., Bradford, P. A., Angulo, F. J., and Hinrichs, S. H. (2000) *N. Engl. J. Med. 342*, 1242−9.
4. Livermore, D. M. (1998) *J. Antimicrob. Chemother. 41* (Suppl. D), 25−41.
5. Matagne, A., Dubus, A., Galleni, M., and Frere, J. M. (1999) *Nat. Prod. Rep. 16*, 1−19.
6. Bush, K. (1999) *Curr. Pharm. Des. 5*, 839−45.
7. Felici, A., Amicosante, G., Oratore, A., Strom, R., Ledent, P., Joris, B., Fanuel, L., and Frere, J. M. (1993) *Biochem. J. 291*, 151−5.
8. Fabiane, S. M., Sohi, M. K., Wan, T., Payne, D. J., Bateson, J. H., Mitchell, T., and Sutton, B. J. (1998) *Biochemistry 37*, 12404−11.
9. Knox, J. R., Moews, P. C., and Frere, J. M. (1996) *Chem. Biol. 3*, 937−47.
10. Massova, I., and Mobashery, S. (1998) *Antimicrob. Agents Chemother. 42*, 1−17.
11. Rychlewski, L., Zhang, B., and Godzik, A. (1999) *Protein Sci. 8*, 614−24.
12. Neuwald, A. F., Liu, J. S., Lipman, D. J., and Lawrence, C. E. (1997) *Nucleic Acids Res. 25*, 1665−77.
13. Melino, S., Capo, C., Dragani, B., Aceto, A., and Petruzzelli, R. (1998) *Trends Biochem. Sci. 23*, 381−2.
14. Concha, N. O., Rasmussen, B. A., Bush, K., and Herzberg, O. (1996) *Structure 4*, 823−36.
15. Carfi, A., Pares, S., Duee, E., Galleni, M., Duez, C., Frere, J. M., and Dideberg, O. (1995) *EMBO J. 14*, 4914−21.
16. Ullah, J. H., Walsh, T. R., Taylor, I. A., Emery, D. C., Verma, C. S., Gamblin, S. J., and Spencer, J. (1998) *J. Mol. Biol. 284*, 125−36.
17. Concha, N. O., Janson, C. A., Rowling, P., Pearson, S., Cheever, C. A., Clarke, B. P., Lewis, C., Galleni, M., Frere, J. M., Payne, D. J., Bateson, J. H., and Abdel-Meguid, S. S. (2000) *Biochemistry 39*, 4288−4298.
18. Sanschagrin, F., Dufresne, J., and Levesque, R. C. (1998) *Antimicrob. Agents Chemother. 42*, 1245−8.
19. Riccio, M. L., Franceschini, N., Boschi, L., Caravelli, B., Cornaglia, G., Fontana, R., Amicosante, G., and Rossolini, G. M. (2000) *Antimicrob. Agents Chemother. 44*, 1229−35.
20. Bellais, S., Poirel, L., Leotard, S., Naas, T., and Nordmann, P. (2000) *Antimicrob. Agents Chemother. 44*, 3028−34.
21. Iyobe, S., Kusadokoro, H., Ozaki, J., Matsumura, N., Minami, S., Haruta, S., Sawai, T., and O'Hara, K. (2000) *Antimicrob. Agents Chemother. 44*, 2023−7.
22. Levinson, W., and Jawetz, E. (2000) *Medical Microbiology & Immunology: Examination & board review*, 6th ed., Lang Medical Books/McGraw-Hill, New York.
23. Bicknell, R., and Waley, S. G. (1985) *Biochemistry 24*, 6876−87.
24. Bicknell, R., Schaffer, A., Waley, S. G., and Auld, D. S. (1986) *Biochemistry 25*, 7208−15.
25. Bounaga, S., Laws, A. P., Galleni, M., and Page, M. I. (1998) *Biochem. J. 331*, 703−11.
26. Wang, Z., Fast, W., and Benkovic, S. J. (1999) *Biochemistry 38*, 10013−23.
27. Wang, Z., and Benkovic, S. J. (1998) *J. Biol. Chem. 273*, 22402−8.
28. Ho, S. N., Hunt, H. D., Horton, R. M., Pullen, J. K., and Pease, L. R. (1989) *Gene 77*, 51−9.
29. O'Callaghan, C. H., Morris, A., Kirby, S. M., and Shingler, A. H. (1972) *Antimicrob. Agents Chemother. 1*, 283−8.
30. Barshop, B. A., Wrenn, R. F., and Frieden, C. (1983) *Anal. Biochem. 130*, 134−45.
31. Dang, Q., and Frieden, C. (1997) *Trends Biochem. Sci. 22*, 317.
32. Paul-Soto, R., Hernandez-Valladares, M., Galleni, M., Bauer, R., Zeppezauer, M., Frere, J. M., and Adolph, H. W. (1998) *FEBS Lett. 438*, 137−40.
33. Pollak, V., and Kuban, M. (1979) *Coll. Czeck. Chem. Commun. 44*, 725−741.
34. Hunt, J. B., Neece, S. H., and Ginsburg, A. (1985) *Anal. Biochem. 146*, 150−7.
35. Hernandez Valladares, M., Kiefer, M., Heinz, U., Paul Soto, R., Meyer-Klaucke, W., Nolting, H. F., Zeppezauer, M., Galleni, M., Frere, J., Rossolini, G. M., Amicosante, G., and Adolph, H. (2000) *FEBS Lett. 467*, 221−5.
36. Kaminskaia, N. V., Spingler, B., and Lippard, S. J. (2000) *J. Am. Chem. Soc. 122*, 6411−22.

37. Kaminskaia, N. V., He, C., and Lippard, S. J. (2000) *Inorg. Chem. 39*, 3365−73.
38. Li, Z., Rasmussen, B. A., and Herzberg, O. (1999) *Protein Sci. 8*, 249−52.
39. Yang, Y., Keeney, D., Tang, X., Canfield, N., and Rasmussen, B. A. (1999) *J. Biol. Chem. 274*, 15706−11.
40. Paul-Soto, R., Zeppezauer, M., Adolph, H. W., Galleni, M., Frere, J. M., Carfi, A., Dideberg, O., Wouters, J., Hemmingsen, L., and Bauer, R. (1999) *Biochemistry 38*, 16500−6.
41. Gensmantel, N. P., Proctor, P., and Page, M. I. (1980) *J. Chem. Soc., Perkin Trans. 2*, 1725−1732.
42. Orellano, E. G., Girardini, J. E., Cricco, J. A., Ceccarelli, E. A., and Vila, A. J. (1998) *Biochemistry 37*, 10173−80.
43. Fitzgerald, P. M., Wu, J. K., and Toney, J. H. (1998) *Biochemistry 37*, 6791−800.
44. Scrofani, S. D., Chung, J., Huntley, J. J., Benkovic, S. J., Wright, P. E., and Dyson, H. J. (1999) *Biochemistry 38*, 14507−14.
45. Bicknell, R., and Waley, S. G. (1985) *Biochem. Soc. Trans. 13*, 766−7.
46. Wang, Z., Fast, W., Valentine, A. M., and Benkovic, S. J. (1999) *Curr. Opin. Chem. Biol. 3*, 614−22.
47. Kiefer, L. L., Paterno, S. A., and Fierke, C. A. (1995) *J. Am. Chem. Soc. 117*, 6831−7.
48. Atanasov, B. P., Mustafi, D., and Makinen, M. W. (2000) *Proc. Natl. Acad. Sci. U.S.A. 97*, 3160−5.
49. Diaz, N., Suarez, D., and Merz, K. M. (2000) *J. Am. Chem. Soc. 122*, 4197−208.
50. Bennett, B., and Holz, R. C. (1997) *J. Am. Chem. Soc. 119*, 1923−33.
51. McManus-Munoz, S., and Crowder, M. W. (1999) *Biochemistry 38*, 1547−53.

BI001860V